EPJ Web of Conferences **146**, 05001 (2017)
*ND2016*

DOI: 10.1051/epjconf/201714605001

# E1 and M1 strength functions at low energy

Ronald Schwengner[1,a], Ralph Massarczyk[1,2], Daniel Bemmerer[1], Roland Beyer[1], Arnd R. Junghans[1], Toni Kögler[1,3], Gencho Rusev[2], Anton P. Tonchev[4], Werner Tornow[5], and Andreas Wagner[1]

[1] Helmholtz-Zentrum Dresden-Rossendorf, 01328 Dresden, Germany
[2] Los Alamos National Laboratory, Los Alamos, New Mexico 87545, USA
[3] Technische Universität Dresden, 01062 Dresden, Germany
[4] Lawrence Livermore National Laboratory, Livermore, California 94550, USA
[5] Triangle Universities Nuclear Laboratory and Duke University, Durham, North Carolina 27708, USA

**Abstract.** We report photon-scattering experiments using bremsstrahlung at the $\gamma$ELBE facility of Helmholtz-Zentrum Dresden-Rossendorf and using quasi-monoenergetic, polarized $\gamma$ beams at the HI$\gamma$S facility of the Triangle Universities Nuclear Laboratory in Durham. To deduce the photoabsorption cross sections at high excitation energy and high level density, unresolved strength in the quasicontinuum of nuclear states has been taken into account. In the analysis of the spectra measured by using bremsstrahlung at $\gamma$ELBE, we perform simulations of statistical $\gamma$-ray cascades using the code $\gamma$DEX to estimate intensities of inelastic transitions to low-lying excited states. Simulated average branching ratios are compared with model-independent branching ratios obtained from spectra measured by using monoenergetic $\gamma$ beams at HI$\gamma$S. E1 strength in the energy region of the pygmy dipole resonance is discussed in nuclei around mass 90 and in xenon isotopes. M1 strength in the region of the spin-flip resonance is also considered for xenon isotopes. The dipole strength function of $^{74}$Ge deduced from $\gamma$ELBE experiments is compared with the one obtained from experiments at the Oslo Cyclotron Laboratory. The low-energy upbend seen in the Oslo data is interpreted as M1 strength on the basis of shell-model calculations.

## 1. Introduction

An improved experimental and theoretical description of photonuclear reactions and their inverse, the radiative-capture reactions, is very important for the description of astrophysical processes, such as the synthesis of heavy nuclei in stellar environments. Gamma-ray strength functions, in particular electric dipole (E1) and magnetic dipole (M1) strength functions, are an important ingredient for the calculation of reaction cross sections within the statistical model. Therefore, precise measurements of dipole strength distributions are needed for a correct determination of those cross sections and for an improvement of theoretical descriptions. Experiments based on photon scattering, also called nuclear resonance fluorescence (NRF), and on light-ion scattering have revealed several previously unknown structures of the absorption cross section and the related dipole-strength function on top of the tail of the isovector giant dipole resonance (GDR) at energies below the neutron-separation energy $S_n$. One of these is the E1 pygmy dipole resonance (PDR). A review of studies of the PDR is given in Ref. [1]. In the energy region, where the spin-flip resonance is expected to occur [2], few examples of an M1 resonance were found in NRF experiments [3,4]. Strong M1 excitations around 3 MeV observed in various NRF studies are considered as the scissors mode [2]. This mode was also identified in light-ion scattering with a total strength exceeding the typical one found in NRF experiments by a factor of about two [5]. A spectacular phenomenon is the observation of an upbend of the strength function at low transition energy in several studies at the cyclotron of Oslo University, which is at variance to the hitherto assumed decreasing strength toward $E_\gamma = 0$. First observed in Mo isotopes [6], the upbend has been found in nuclides in several other regions of the nuclear chart. The latest observations are discussed in Refs. [7–9]. In a recent experiment using the (p,d) reaction, the upbend as well as the scissors resonance were observed in $^{153,155}$Sm [10]. A physical explanation of the upbend has been given on the basis of shell-model calculations [11,12]. These calculations show that large M1 strengths are produced for transitions between close-lying states by recoupling the spins of high-$j$ orbits [11].

In the present work, we report photon-scattering experiments and results for the E1 strength in the PDR region, M1 strength in the spin-flip region and low-energy M1 strength.

## 2. Experiments

Photon-scattering experiments were carried out using bremsstrahlung at the $\gamma$ELBE facility [13] of Helmholtz-Zentrum Dresden-Rossendorf (HZDR), Germany, and using quasimonoenergetic, highly polarized $\gamma$ beams at the High-Intensity $\gamma$-Ray Source (HI$\gamma$S) [14] operated by the Triangle Universities Nuclear Laboratory (TUNL) in Durham, North Carolina, USA.

To deduce absolute photoabsorption cross sections, the experimental spectra have to be corrected for the detector

---

[a] e-mail: `r.schwengner@hzdr.de`

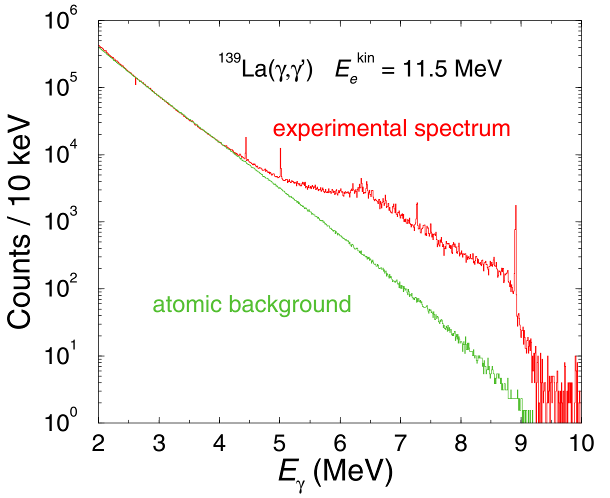

**Figure 1.** Response-corrected experimental spectrum measured in the $^{139}$La($\gamma$, $\gamma'$) experiment at $\gamma$ELBE and simulated spectrum of atomic background, multiplied with efficiency and measuring time. Taken from Ref. [16].

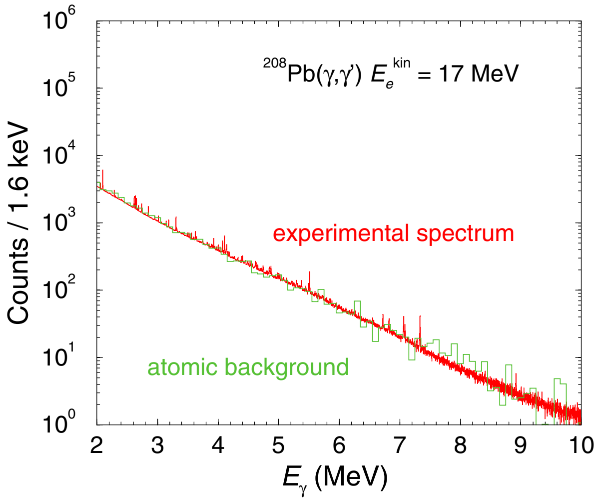

**Figure 2.** Response-corrected experimental spectrum measured in the $^{208}$Pb($\gamma$, $\gamma'$) experiment at $\gamma$ELBE and simulated spectrum of atomic background, multiplied with efficiency and measuring time.

response. For this purpose, spectra of monoenergetic $\gamma$ rays are calculated in steps of 10 keV by using the code GEANT4 [15]. Starting from the high-energy end of the spectrum, the simulated spectra are subtracted sequentially (spectrum-strip method). When analyzing spectra at high excitation energy and thus high level density, unresolved strength in the quasicontinuum of nuclear states has to be taken into account. To determine the intensity in the nuclear quasicontinuum, the spectrum of $\gamma$ rays scattered from the target in atomic processes is simulated by using the code GEANT4 and subtracted from the response-corrected experimental spectrum. The contributions of unresolved strength to the spectra are demonstrated for the nuclides $^{139}$La [16] and $^{208}$Pb [17] in Figs. 1 and 2, respectively. One sees that there is a considerable amount of intensity in the quasicontinuum above the atomic background in the spectrum of $^{139}$La, which has a high level density, whereas the atomic background coincides with the continuum in the spectrum of $^{208}$Pb, which has a very small level density, and there is negligible intensity left for the nuclear quasicontinuum.

In the analysis of the spectra measured by using bremsstrahlung at $\gamma$ELBE, simulations of statistical $\gamma$-ray cascades using the code $\gamma$DEX [18–20] are performed to estimate intensities of branching transitions to low-lying excited states. In these simulations, level densities with parameters taken from Ref. [21] and a parity distribution of the level densities according to Ref. [22] are used. For the input strength functions, phenomenological expressions provided by the RIPL-3 data base [23] are applied. Simulated average branching ratios of ground-state transitions are compared with model-independent experimental branching ratios obtained from spectra measured by using monoenergetic $\gamma$ beams at HI$\gamma$S in Fig. 3. The simulated and experimental branching ratios agree within their uncertainties, which serves as a proof of the reliability of the cascade simulations. Absorption cross sections are deduced by applying the simulated average branching ratios of the ground-state transitions.

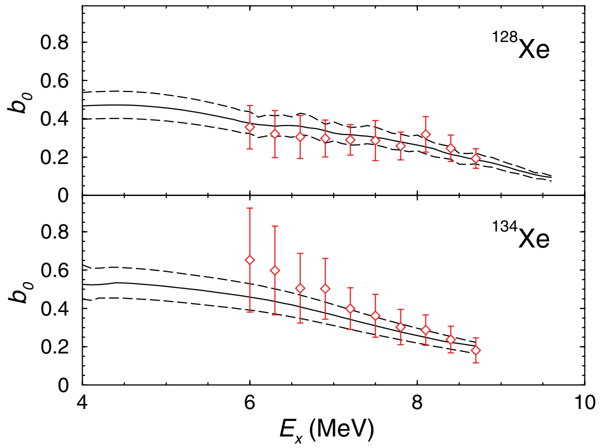

**Figure 3.** Branching ratios of ground-state transitions in $^{128}$Xe and $^{134}$Xe deduced from experiments at HI$\gamma$S (red diamonds) and obtained from $\gamma$-ray cascade simulations (black solid lines) with their uncertainties (black dashed lines). Taken from Ref. [4].

## 3. Results

In several nuclides around mass $A = 90$, we found extra strength considered as a PDR on top of the low-energy tail of the GDR. As an example, the results of the $\gamma$ELBE experiment for $^{86}$Kr [24] are shown in Fig. 4. For comparison, $^{86}$Kr($\gamma, n$) data obtained in a HI$\gamma$S experiment [25] and the curve corresponding to the three-Lorentzian model [26] are shown. The extra strength in the PDR region is similarly pronounced in the neighboring $N = 50$ isotones and is qualitatively reproduced in calculations based on the quasiparticle-phonon model [24].

To study the influence of properties such as neutron excess and nuclear deformation on the dipole strength in the PDR region, we investigated the series of Xe isotopes in experiments at $\gamma$ELBE and at HI$\gamma$S. We found that the dipole strength develops with the neutron excess, whereas the deformation has a minor influence [20].

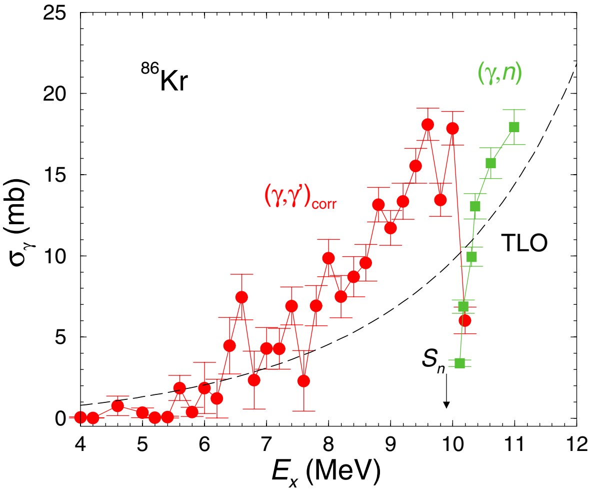

**Figure 4.** Absorption cross sections of $^{86}$Kr as obtained from $(\gamma,\gamma')$ experiments, including strength in the quasicontinuum and corrected for branching intensities (red circles), in comparison with $(\gamma,n)$ data (green squares) and the three-Lorentzian model (black dashed line). Taken from Ref. [24].

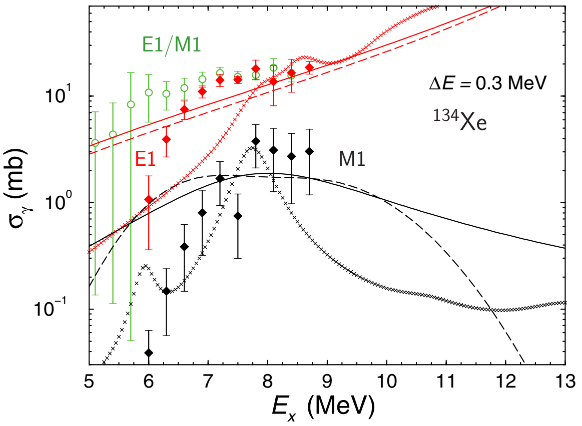

**Figure 5.** Photoabsorption cross sections for $^{134}$Xe deduced from experiments at HI$\gamma$S for the E1 part (red diamonds) and the M1 part (black diamonds). For comparison, data from our experiment at ELBE [20] including both, E1 and M1 contributions, in 0.3 MeV bins are shown (green circles). In addition, predictions of phenomenological expressions are given. RIPL3 [23] recommendations for the E1 and M1 parts are plotted as red and black solid curves, respectively. The TLO model [26] for E1 and a triple-Gaussian model according to Ref. [2] for M1 are shown as red and black dashed curves, respectively. Red and black crosses represent the result of QRPA calculations for the E1 and M1 strength, respectively. Taken from Ref. [4].

The experiments with polarized $\gamma$ beams at HI$\gamma$S allowed us to distinguish between E1 strength and M1 strength. The results for $^{134}$Xe are shown in Fig. 5. One sees that the M1 strength amounts to some 10% of the E1 strength in the energy region between about 6 and 9 MeV. The M1 data may indicate a resonance-like structure at about 8.5 MeV, which is the energy region of the spin-flip resonance. A similar behavior is predicted by QRPA calculations [4].

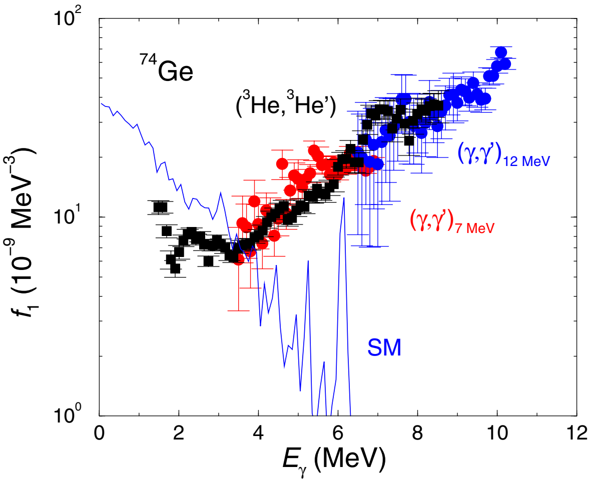

**Figure 6.** Dipole strength functions of $^{74}$Ge based on $(\gamma,\gamma')$ data measured at two electron energies of 7 MeV (red circles) and 12 MeV (blue circles) and based on ($^3$He,$^3$He') data (black squares). The M1 strength function deduced from shell-model calculations is also shown (blue solid line). $(\gamma,\gamma')$ data are from Ref. [27] and ($^3$He,$^3$He') data from Ref. [8].

The nuclide $^{74}$Ge has been chosen as a test case for the consistency of strength functions deduced from experiments using different reactions. We have studied $^{74}$Ge via the $(\gamma,\gamma')$ reaction at $\gamma$ELBE [27]. Besides, the dipole strength function of $^{74}$Ge was extracted from experiments using the ($^3$He,$^3$He') reaction at the cyclotron of Oslo University [8] and relative cross sections were obtained from an $(\alpha,\alpha')$ experiment at the cyclotron of iThemba LABS Somerset [28].

The strength function is deduced from the photoabsorption cross section $\sigma_\gamma$ determined in $(\gamma,\gamma')$ experiments using the relation $f_1 = \sigma_\gamma/[g(\pi\hbar c)^2 E_\gamma]$ with $g = (2J_i+1)/(2J_0+1)$, where $J_0$ and $J_i$ are the spins of the ground state and the excited state, respectively. The strength function derived in this way for $^{74}$Ge is compared with the one obtained from ($^3$He,$^3$He') experiments in Fig. 6. We analyzed two $(\gamma,\gamma')$ data sets from measurements at electron energies of 7 and 12 MeV, respectively. The correction of the data for branching ratios was applied separately to the two sets and allowed us to extend the correction of the photoabsorption cross section to low energy. There is a good agreement between the $(\gamma,\gamma')$ and ($^3$He,$^3$He') data in the transition-energy region from about 4 to 9 MeV. The uncertainties of the $(\gamma,\gamma')$ data become very large below about 3 MeV even for the 7 MeV experiment. In addition to the limitation based on the step-by-step correction procedure, cross sections at very low energy cannot be derived from photon scattering because of missing states for the excitation and subsequent deexcitation via $\gamma$ transitions. In contrast, the ($^3$He,$^3$He') data reach to low energies of about 1.5 MeV. Whereas the energy of the $\gamma$ transition is equal to the excitation energy in measurements using the $(\gamma,\gamma')$ reaction, close-lying states at high excitation energy can be populated in light-ion scattering experiments that are connected by transitions of very small energy. In analogy to earlier experiments mentioned in Sect. 1, an upbend of the strength function toward low energy below about 2 MeV is observed in the ($^3$He,$^3$He') data. This upbend has been explained on the basis of shell-model calculations as caused by large M1 strengths of transitions between close-lying states with analogous configurations, in which the involved proton and neutron orbits recouple their spins [11,12]. An M1 strength function based on shell-model calculations for $^{74}$Ge is also shown in Fig. 6. This strength function was extracted from about 23,800 M1 transitions between the lowest 40 states each for all spins up to 10 [8]. The low-energy enhancement of M1 strength found in the calculations describes qualitatively the observed upbend, but exceeds the experimental data by about a factor of two.

## 4. Summary

We described photon-scattering experiments with bremsstrahlung at $\gamma$ELBE and with quasi-monoenergetic and polarized $\gamma$ rays at HI$\gamma$S. We included strength in the quasicontinuum in the analysis of the $\gamma$-ray intensities. Besides, we corrected the intensities measured in experiments with bremsstrahlung for branching and feeding by means of statistical methods. A comparison of simulated branching ratios of ground-state transitions with model-independent ones determined from spectra measured with monoenergetic $\gamma$ beams at HI$\gamma$S proves the reliability of the statistical $\gamma$-ray cascade simulations.

The present experiments gained novel experimental information about E1 strength in the pygmy region and M1 strength in the spin-flip region.

We derived M1 strength functions from large numbers of M1 transition strengths calculated within the shell model. These M1 strength functions describe the low-energy upbends of the strength functions observed in various light-ion scattering experiments.

### References

[1] D. Savran, T. Aumann, and A. Zilges, Prog. Part. Nucl. Phys. **70**, 210 (2013)
[2] K. Heyde, P. von Neumann-Cosel, A. Richter, Rev. Mod. Phys. **82**, 2365 (2010)
[3] G. Rusev et al., Phys. Rev. Lett. **110**, 022503 (2013)
[4] R. Massarczyk, G. Rusev, R. Schwengner, F. Dönau, C. Bhatia, M.E. Gooden, J.H. Kelley, A.P. Tonchev, and W. Tornow, Phys. Rev. C **90**, 054310 (2014)
[5] M. Guttormsen et al., Phys. Rev. Lett. **109**, 162503 (2012)
[6] M. Guttormsen et al., Phys. Rev. C **71**, 044307 (2005)
[7] A.C. Larsen et al., Phys. Rev. C **93**, 045810 (2016)
[8] T. Renstrøm et al., Phys. Rev. C **93**, 064302 (2016)
[9] G.M. Tveten et al., Phys. Rev. C **94**, 025804 (2016)
[10] A. Simon et al., Phys. Rev. C **93**, 034303 (2016)
[11] R. Schwengner, S. Frauendorf, and A. C. Larsen, Phys. Rev. Lett. **111**, 232504 (2013)
[12] B.A. Brown and A.C. Larsen, Phys. Rev. Lett. **113**, 252502 (2014)
[13] R. Schwengner et al., Nucl. Instr. Meth. A **555**, 211 (2005)
[14] H.R. Weller et al., Prog. Part. Nucl. Phys. **62**, 257 (2009)
[15] S. Agostinelli et al., Nucl. Instr. Meth. A **506**, 250 (2003)
[16] A. Makinaga et al., Phys. Rev. C **82**, 024314 (2010)
[17] R. Schwengner et al., Phys. Rev. C **81**, 054315 (2010)
[18] G. Schramm et al., Phys. Rev. C **85**, 014311 (2012)
[19] R. Massarczyk et al., Phys. Rev. C **86**, 014319 (2012)
[20] R. Massarczyk et al., Phys. Rev. Lett. **112**, 072501 (2014)
[21] T. von Egidy and D. Bucurescu, Phys. Rev. C **80**, 054310 (2009)
[22] S. I. Al-Quraishi, S. M. Grimes, T. N. Massey, and D. A. Resler, Phys. Rev. C **67**, 015803 (2003)
[23] R. Capote et al., Nucl. Data Sheets **110**, 3107 (2009)
[24] R. Schwengner et al., Phys. Rev. C **87**, 024306 (2013)
[25] R. Raut et al., Phys. Rev. Lett. **111**, 112501 (2013)
[26] A. R. Junghans, G. Rusev, R. Schwengner, A. Wagner, and E. Grosse, Phys. Lett. B **670**, 200 (2008)
[27] R. Massarczyk et al., Phys. Rev. C **92**, 044309 (2015)
[28] D. Negi et al., Phys. Rev. C **94**, 024332 (2016)